Low-temperature behavior of core-softened models: Water and silica behavior

E. A. Jagla
Centro Atómico Bariloche and Instituto Balseiro, Comisión Nacional de Energía Atómica, (8400) S. C. de Bariloche, Argentina
(Received 29 December 2000; published 29 May 2001)

A core-softened model of a glass forming fluid is numerically studied in the limit of very low temperatures. The model shows two qualitatively different behaviors depending on the strength of the attraction between particles. For no or low attraction, the changes of density as a function of pressure are smooth, although hysteretic due to mechanical metastabilities. For larger attraction, sudden changes of density upon compressing and decompressing occur. This global mechanical instability is correlated to the existence of a thermodynamic first-order amorphous-amorphous transition. The two different behaviors obtained correspond qualitatively to the different phenomenology observed in silica and water.

DOI: 10.1103/PhysRevE.63.061509 PACS number(s): 64.70.Ja, 61.20.−p, 61.20.Ja

I. INTRODUCTION

The recently acknowledged possibility of the existence of single component systems which display coexistence between two different liquid phases has opened many interesting questions, and shed new light into the study of the anomalous properties these systems display [1–3]. The case of water is probably the most intensively studied, due to its ubiquity in nature. There is by now a general consensus that water displays a transition between two different amorphous states in the supercooled region of its phase diagram [4]. Experiments carried out in water at $T \simeq 130$ K show an abrupt change of volume v as a function of pressure P, which indicates the existence of the first order transition [5]. The $v(P)$ curve is hysteretic, and the jump in v occurs at $P \simeq 0.3$ GPa upon compressing, and at $P \simeq 0.05$ GPa upon decompressing. The volume change at the transition is about 0.2 cm^3/g. The two amorphous phases of water are smoothly related to two different liquid phases at higher temperatures, which at coexistence determine a first order liquid-liquid transition line ending in a critical point, located in the metastable region of the phase diagram. Most of the anomalies of water are usually interpreted as a consequence of the existence of this liquid-liquid line and the liquid-liquid critical point, but in general the existence of liquid-liquid coexistence is not a necessary condition for the existence of most of the anomalies [6].

Water is not an isolated case. There is a whole family of substances, usually referred to as tetrahedrally coordinated materials, that display many of the anomalies of water [7]. Within this family, another particularly interesting case is that of amorphous SiO_2 (silica). Many of the anomalous properties of water are also found in silica. Some of them have been observed in experiments (as the density anomaly) and others only in numerical simulations up to now (as maxima of isothermal compressibility and diffusivity as a function of pressure [8]). This has led to think that possibly a first-order amorphous-amorphous transition also occurs in silica. But evidence of this transition has been elusive. Experiments at ambient temperature in silica show an irreversible increase of density when the system is compressed up to $P \gtrsim 20$ GPa and successively decompressed [9]. This behavior is reproduced in numerical simulations [10]. However, for no particular value of pressure there is a sudden change in density that could be interpreted as a direct evidence of a first-order transition.

It has been argued that the qualitatively different behavior of water and silica is due to the temperature at which experiments are carried out compared to the glass temperature T_g of the materials [11,8,12]. Whereas T/T_g is about 0.1 for the experiments in silica, it is close to 1 for water. Some people have raised the expectation that if compressing experiments were done in silica at temperatures near or above T_g, they would reveal the first-order transition, which is supposed to be hidden in the ambient temperature experiments due to lack of thermodynamic equilibrium.

We will not study the actual behavior of water and silica, nor even of the numerical models that have been used to simulate then. Instead, we will study a very simple model of a glass former at low temperatures, including the limiting $T=0$ case, in different regions of the parameters to gain qualitative insight into the problem. The model consists of particles interacting through a potential with a hard core plus a soft repulsive shoulder. In addition, an attractive contribution to the interaction can be included. This kind of model is not unrealistic for the study of the properties of tetrahedrally coordinated materials, and in fact it was shown to reproduce many of the anomalies these materials possess [6,13]. We will show that when there is no attraction between particles (or only a weak one), implying in particular that there is no first order transition, the $v(P)$ curve of our model in simulations at $T=0$ shows an hysteretic behavior, which is associated to the existence of different mechanically stable configurations, and qualitatively agrees with the known phenomenology of silica. The inclusion of a sufficiently strong attraction may produce the appearance of a first-order transition, which is clearly observed even in simulations at $T=0$, in the form of a global mechanical instability. The form of $v(P)$ we obtain in this case is very similar to what is found in water.

These findings will lead us to propose a different scenario to place together the properties of water and silica. We suggest that the first-order transition in water will be observed in the form of a mechanical instability even in experiments at $T \to 0$. On the other hand, we suggest the possibility that a first-order transition in silica is not observed because there is

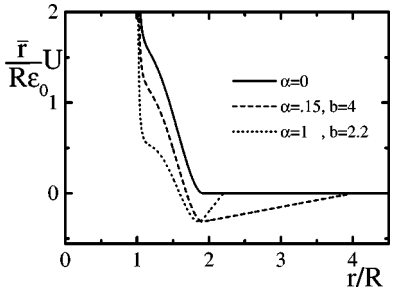

FIG. 1. The interparticle potential $U(r)$ without attraction (continuous line) and for two different choices of the attractive part. In this plot, the value $R=\overline{r}$ was assumed.

not one, and that experiments performed in silica near T_g will not reveal new qualitative ingredients. It is worth noticing that the existence of the thermodynamic anomalies of silica does not contradict this interpretation, since a liquid-liquid critical point is not necessary to observe those anomalies, as it is known from studies in models closely related to the present one [6].

The paper is organized as follows. The model and details on the simulation procedure are presented in Sec. II. The results are contained in Sec. III, and the relevance of them to silica and water is presented in Sec. IV. Section V contains the summary and some final comments.

II. THE MODEL

The model we study is defined as follows. We consider a bidisperse set of spherical particles, in order to avoid crystallization. Particle i is characterized by the value of a parameter r_i, which is taken from a bimodal distribution, i.e., $r_i=r_a$, or $r_i=r_b$, with equal probability. The interaction potential U between particles i and j depends on $\tilde{r}\equiv r/R$ where r is the real distance between particles, and $R=r^i+r^j$. The potential U is composed of a repulsive and an attractive part, $U\equiv U^R+U^A$. The form we use for U^R is

$$U^R=\infty \quad \text{for} \quad \tilde{r}<1,$$

$$U^R=\varepsilon_0\frac{R}{r}\left(\frac{0.01}{\tilde{r}-1}+1.2-1.8(\tilde{r}-1.1)^2\right)^2$$

$$\text{for} \quad 1<\tilde{r}<1.9202,$$

$$U^R=0 \quad \text{for} \quad \tilde{r}>1.9202, \tag{1}$$

where $\overline{r}$ is the mean radius of the particles. U^R is plotted in Fig. 1. The form of this potential is a smooth version of a potential that we have studied in detail previously [6,14]. This smoother form is preferred here in order to avoid ambiguities in the calculations at $T=0$, that appear in case the forces are not continuous. The particular analytical form we use is not really important, the only crucial feature of the potential is the existence of two preferred distances between particles ($r_0\sim 1.1\,R$ and $r_1\sim 1.9\,R$ in Fig. 1) depending on the value of the external pressure. The attractive part of the potential U^A is simply given by

$$U^A=\varepsilon_0\frac{R}{r}\alpha(\tilde{r}-b) \quad \text{for} \quad \tilde{r}<b,$$

$$U^A=0 \quad \text{for} \quad \tilde{r}>b. \tag{2}$$

with the two dimensionless parameters b and α fixing, respectively, the range and intensity of the attraction. Two examples of the potential with the attraction term (those to be used in the simulations) are also shown in Fig. 1. In all the results to be presented (corresponding to two-dimensional systems), we use $r_a=0.45\overline{r}$, and $r_b=0.55\overline{r}$. Temperature will be measured in units of $\varepsilon_0 k_B^{-1}$, pressure in units of $\varepsilon_0 k_B^{-1}\overline{r}^{-2}$, and volume in units of $\overline{r}^2$.

We simulate the system by standard Monte Carlo techniques, using Metropolis algorithm. Particles are placed in a box with periodic boundary conditions. At each time step the position of a single particle is modified to a new position which is randomly chosen within a sphere of radius $0.01\,\overline{r}$ centered at the original position. This trial movement is accepted according to the Metropolis rule. The update is made sequentially for all particles. Results using constant pressure simulations and others at constant volume will be shown. In the constant pressure scheme, the volume of the system is considered as an additional Monte Carlo variable, and homogeneous expansion and contraction of the coordinates of all particles (and also of the size of the simulation box) are tried. This permits the volume of the system to adjust to the given external pressure. In constant volume simulations, pressure is calculated as minus the energy change divided the volume change in a small (virtual) homogeneous rescaling of all coordinates of the particles.

III. RESULTS

We will show results for a two-dimensional system. This is done to allow a better visualization of the configurations, however we emphasize that all the results we discuss were qualitatively reobtained in three-dimensional systems. We start by showing results in the case of no attraction ($\alpha=0$), at $T=0$. Note that $T=0$ Monte Carlo means that trial movements of the particles are accepted if and only if they do not increase the energy of the system. Particles are randomly placed in space at the beginning of the simulation, and the system is rapidly compressed up to reaching a mechanically stable configuration at $P\sim 0.5$, $v\sim 3.2$. Then P is increased, or v is decreased (depending on the type of simulations) by small steps. Mechanical equilibrium is obtained at each P-v value. In this way we reach $P\sim 4$, $v\sim 1.5$. Then we slowly expanded the system to the original values of P and v.

We see in Fig. 2 the values of P and v during this process, both in simulations at constant P an at constant v for a system of 200 particles. The curves show a series of small though abrupt changes in v or P (depending on the kind of simulations) that correspond to mechanical instabilities in the system [15]. Also the hysteresis in $v(P)$ we observe (which

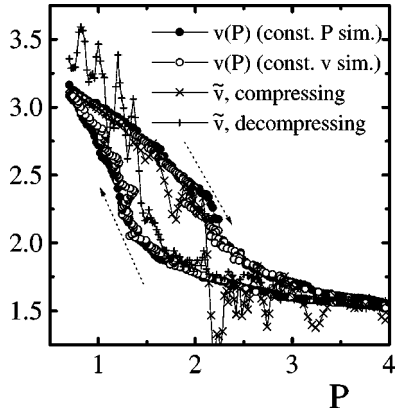

FIG. 2. $v(P)$ function for the system without attraction, at $T=0$. Results of simulations at constant P and constant v are shown. Also shown are the values of $\tilde{v}\equiv\partial h/\partial P$, from the constant P simulations. Differences between v and $\tilde{v}$ reveal lack of thermodynamic equilibrium. Pressure is given in units of $\varepsilon_0 k_B^{-1}\overline{r^{-2}}$, and volume in units of $\overline{r^2}$.

we found is repetitive upon compressing and decompressing, though only one cycle is shown in Fig. 2) originates in the existence of mechanical metastabilities in the system. An indication of this fact can be obtained from the following arguments. Let us define $\tilde{v}\equiv\partial h/\partial P$, where $h=e+Pv$ is the enthalpy per particle of the system as obtained from the simulations. If the system was in thermodynamic equilibrium we should obtain $\tilde{v}=v$, since this is a thermodynamic identity at $T=0$. We plot $\tilde{v}$ (from the constant P simulations) also in Fig. 2. We see that there are systematic differences between v and $\tilde{v}$, particularly in the region where v changes rapidly. The difference between v and $\tilde{v}$ is due to mechanical instabilities upon compressing and decompressing that produce energy to be dissipated in the process. A very simple example is illuminating in this respect. For two particles interacting with the potential of Fig. 1 (continuous line) at $T=0$, the evolution of distance d (that replaces volume in this case) and enthalpy h as a function of the compressing force F (that takes the role of pressure) is shown in Fig. 3. The mechanical hysteresis in $d(F)$ is precisely the same effect we observe in the simulations, the only difference is that in the

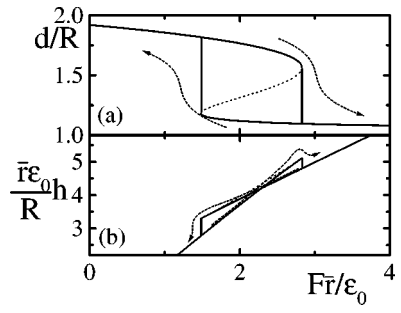

FIG. 3. Distance d (a) and enthalpy $h\equiv U+Fd$ (b) for two particles interacting with the potential of Fig. 1 (continuous line) as a function of the compressing force F. Compressing and decompressing routes are indicates.

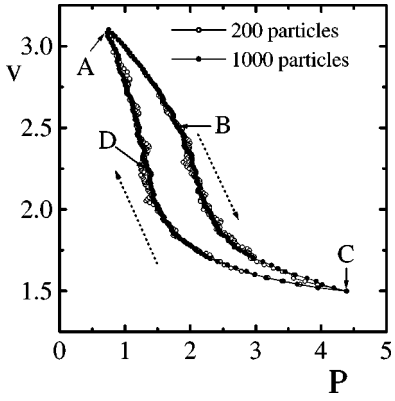

FIG. 4. $v(P)$ curve as in Fig. 2, for systems with 200 and 1000 particles. Fluctuations tend to average out in the larger sample, but the overall hysteresis remains the same as in the case with fewer particles. Units as in Fig. 2.

simulations the disordered nature of the system produces a smoothing of $v(P)$. In the two particle problem $\tilde{d}\equiv\partial h/\partial F$ equates d except by the existence of two delta peaks at the points where there is a jump in h. This is the energy being dissipated. In the numerical simulations there is an averaging over many different atomic environments, and the delta peaks are smoothed, but still clearly visible as regions where $\tilde{v}<v$ during compressing, or $\tilde{v}>v$ during decompressing in Fig. 2.

The mechanical instabilities in the system are of a local nature, in the sense that they produce noncorrelated rearrangements of particles as pressure or volume changes. Then we expect the small reentrances in the constant v simulations that signal the existence of these instabilities to become weaker in larger samples, since they are averaged over the whole system. In fact, as an indication of this, we show in Fig. 4 results for a system of 1000 particles, as compared to the case of 200 particles, and we see that ''fluctuations'' are considerably smaller. The global amount of hysteresis, however, remains quite the same. Figure 5 shows snapshots of the 1000 particles system at the points indicated in Fig. 4. Figure 6 shows the corresponding radial distribution function. We see that as the pressure increases and volume de-

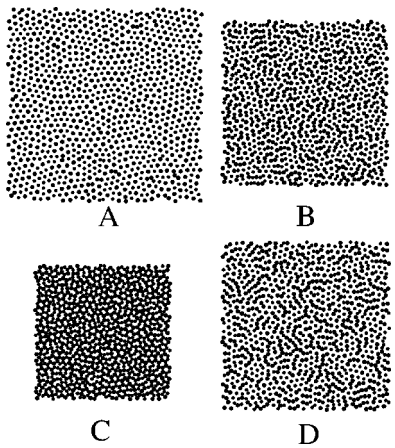

FIG. 5. Snapshots of the system at the points indicated in Fig. 4. Dot size represents the hard core of the particles.

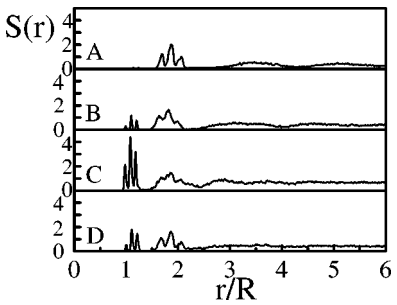

FIG. 6. Radial distribution functions $S(r)$ (in units of $\overline{r^{-2}}$) of the configurations shown in Fig. 5. The weight transfer between $r_0 \sim 1.1R$ and $r_1 \sim 1.9R$ is clearly visible (the triplet structure of the peaks originates in the bidispersity of the system).

creases more and more particles move from a typical distance $r_1 \sim 1.9R$ between neighbors to the shorter distance $r_0 \sim 1.1R$. The collapse of neighbor particles from r_1 to r_0 is not a collective effect, it occurs in a noncorrelated way in different positions of the sample, namely, no abrupt transition exists.

From the two particle problem we see an interesting characteristic of the $h(F)$ curve. The values of h in the compressing and decompressing branches cross each other (at $F\overline{r}/\varepsilon_0 \sim 2.3$). This crossing is also observed in the complete simulations. In fact, in Fig. 7 we see values of h obtained during compression and decompression, in the simulations at constant P (all results are for a system of 1000 particles, from now on). We see clearly a crossing of the two branches at about $P \simeq 1.8$. This crossing has no profound physical meaning, and in particular it does not indicate the existence of a first order transition between compressing and decompressing branches, since these are not the thermodynamic values of the free energy, and the states accessed during compression and decompression do not exhaust the whole phase space of the system. To show this in more detail, we made simulations in which the system was annealed at fixed volume, trying to get as closer as possible to the real ground state of the system at each P. The final values of v that we get as $T \to 0$ at different P are shown in Fig. 8. Although we cannot guarantee that the true ground state was obtained, the values of $h(P)$ in this case are systematically lower than both the compression and decompression ones, as we can see

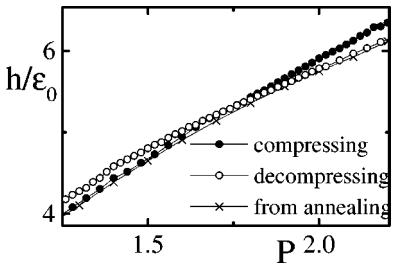

FIG. 7. Evolution of enthalpy h as a function of pressure during compression and decompression, and from individual simulations annealing the system at fixed pressure. Compressing and decompressing branches cross each other at $P \sim 1.8$, but the thermodynamic values are always lower.

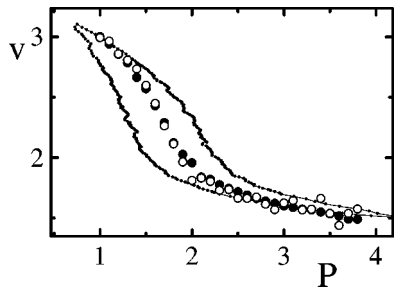

FIG. 8. $v(p)$ curve obtained as the limit $T \to 0$ of individual simulations at constant volume (large full symbols), and calculated $\tilde{v} \equiv \partial h/\partial P$ from the h values obtained in the same simulations (open symbols). Within the numerical errors we get $v = \tilde{v}$, is it should be in thermodynamic equilibrium. The compressing-decompressing loop of Fig. 4 is also shown to allow comparison. Units as in Fig. 2.

in Fig. 7. For the values of $v(P)$ obtained in the annealing simulations, the thermodynamic relation $v = \partial h/\partial P$ is well satisfied within the numerical errors (Fig. 8). The values of $v(P)$ obtained in the annealing process are inside the loop of compression-decompression, as it could be expected for the equilibrium values, since the hysteresis loop represents the maximum amount of mechanical metastability that the system is able to sustain. In addition, $v(P)$ is continuous, and this is consistent with the lack of a thermodynamic first-order transition at $T = 0$ in our model.

To obtain a thermodynamic first-order transition, and to study the way in which it reflects in the compression decompression results at $T = 0$, a certain amount of attraction between particles must be included. The existence of attraction in the system may have profound effects in its phase behavior. We will first discuss analytically the case in which an attraction energy $\gamma(r) < 0$ of infinite range is added to the interparticle energy U included. In this case, the energy per particle e gets an additional contribution δe of the form $\delta e = \int_V S(r)\gamma(r)d\mathbf{r}$, $S(r)$ being the radial distribution function. The assumed limit in which the range of $\gamma(r)$ goes to infinity, corresponds to the case in which this integral is governed only by the limiting value of $S(r)$ as $r \to \infty$, i.e., it will depend only on the density of the system. In this case, $S(r)$ itself is not affected by the attraction term. Then δe takes the form $\delta e = -\tilde{\gamma}/v$ with some constant $\tilde{\gamma} > 0$. This term is directly added to the free energy G of the system. When computing the equation of state from $\partial G/\partial v = 0$, the only difference with the case without attraction is that P in the state equation is replaced by $P + \tilde{\gamma}/v^2$. Then from the results of the simulations without attraction we can immediately get those for a system with an attraction that has infinite range, just rescaling (self-consistently) the pressure axis through $P \to P + \tilde{\gamma}/v^2$. The result of this procedure is shown in Fig. 9. We see that due to the volume-dependent rescaling of P, and to the form of the $v(P)$ curve with no attraction, a reentrance in $v(P)$ may appear if the attraction is higher than some minimum. The reentrance in the thermodynamic $v(P)$ curve indicates the existence of a first-order transition between two amorphous phases of different densities. This reentrance appears also for the compressing and decompressing branches,

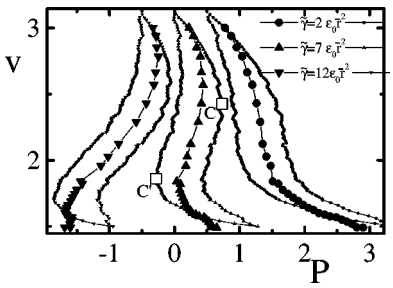

FIG. 9. The effect of an infinite range attraction of different intensities on the $v(P)$ curves of Fig. 8. A reentrance, indicative of a first-order transition is observed for the two largest values of $\tilde{\gamma}$. For $\tilde{\gamma}\simeq 9$ the first-order transition is moved into the metastable $P<0$ region. Large symbols are the (almost) thermodynamic values, and small symbols are the compressing and decompression results. The position of the spinodal points C and C' upon compression and decompression is also shown in the case $\tilde{\gamma}=7$. Units as in Fig. 2.

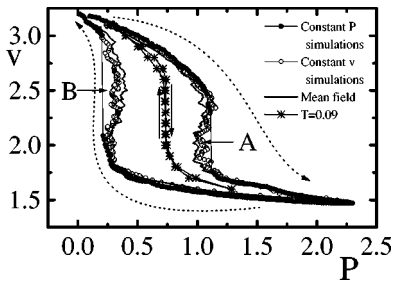

FIG. 10. Full simulations with an attraction term of the form (2) with $b=4$, and $\alpha=0.15$. Constant pressure and constant volume simulations are shown. The mean field result (infinite range attraction) with $\tilde{\gamma}=3.1\varepsilon_0\overline{r^2}$ is shown for comparison. Note the abrupt v change in the constant P simulations, and the weak reentrances of the constant v simulations. These are mechanical instabilities that indicate the existence of a thermodynamic first-order amorphous-amorphous transition in this case, which is made evident in the equilibrium $v(P)$ curve at $T=0.09$. Units as in Fig. 2.

basically at the same value of $\tilde{\gamma}$. This means that in this case the mechanical instability at zero temperature exist if and only if the system has a thermodynamic first-order transition at $T=0$. Then the global mechanical instability upon compression and decompression as pressure passes through the spinodal points at which $\partial v/\partial p$ becomes infinity (points C and C' in Fig. 9) is an indirect observation of the first-order transition. We emphasize that in the present case the instability is global, in the sense that once it occurs, it involves a finite fraction of the whole system, contrary to instabilities in the case without attraction, which are associated to individual particles. We note that for a truly infinite range attraction (more precisely, if the range of the attraction is much larger than the system size) the loop in $v(P)$ when there is a first-order transition is physical, namely, it is observable in constant volume simulations, and no Maxwell construction can be invoked to flatten it out. In constant P simulations instead, we would get an abrupt volume change when we go through the pressure corresponding to the spinodal points, and this is what we are referring to as a global mechanical instability. From Fig. 9 we also see that the position of the first-order loop moves towards lower pressures as the strength of the attraction is increased, and then it can be completely moved into the metastable $P<0$ region when the attraction is strong enough. Notice also that in cases in which the compressibility anomaly of the purely repulsive model (the rapid change in volume around $P\sim 2$ in our case) is weaker, it may happen that no first-order transition appears at all, for any value of the attraction.

The previous analysis tells us that in the case of a long range attraction, the existence of a first-order thermodynamic transition and mechanical instabilities in the compression-decompression path at $T=0$ are closely related, each of them implying the existence of the other. We want to analyze now to what extent this scenario can be extended to the case in which the attraction is short ranged. Then we conducted compressing-decompressing simulations using the finite range form (2) of the attraction. We first use a rather large value $b=4$ for the attraction range, expecting to reobtain basically the mean field phenomenology. For weak attraction [$\alpha\lesssim 0.1$ in Eq. (2)], we get $v(P)$ curves which are slightly modified with respect to the case of no attraction, but no qualitatively new results appear. But if the attraction is strong enough, we obtain signs of global mechanical instabilities and a first-order transition. The results of compression-decompression simulations are illustrated in Fig. 10 for $\alpha=0.15$. We see that constant v simulations get a region (for $1.8<v<2.4$ upon compression) with small reentrances in the calculated values of P. In turn, in constant P simulations we see an abrupt collapse of volume that jumps in a finite amount. This jump signals the occurrence of a global mechanical instability. For comparison, we also plot in Fig. 10 the results of the mean field case, with an infinite range attraction with $\tilde{\gamma}=3.1\varepsilon_0\overline{r^2}$. We can see that the mean field result is quite similar to the numerical result at constant volume. The effect of the finite range attraction can be seen, however, in the snapshots of the system when going through the coexistence region (Fig. 11). Indeed, they show bubbles of the denser amorphous phase appearing in the system as volume is reduced. This does not happen in the mean field case. Note the difference between the configurations in Fig. 11, and those with no attraction during compression and decompression [Figs. 5(B) and 5(D)]. Here the particles that collapse to the new phase tend to form well defined clusters in the sample, whereas in the other case the system remains uniform.

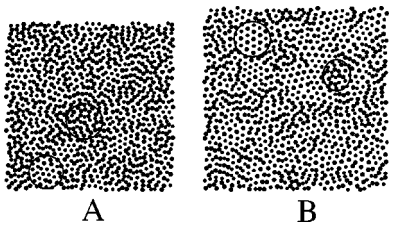

FIG. 11. Snapshots of the system at the points indicated in Fig. 10. Note the coexistence of rather large clusters of two different phases with different densities, as for instance in the encircled regions (compare with Fig. 5).

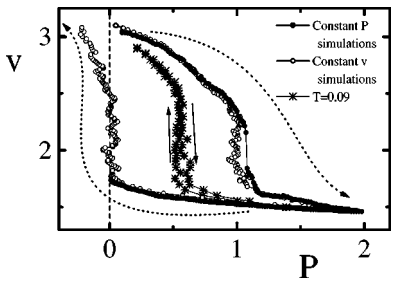

FIG. 12. Same as Fig. 10, but for $b=2.2$, and $\alpha=1.0$ (see Fig. 1 for a sketch of the potential).

In this case in which the attraction range is rather large we expect the mean field arguments of the previous section to apply, and then that the system has (in addition to the global mechanical instabilities at zero temperature) a thermodynamic phase transition at sufficiently low temperatures. To check directly for this transition is of course not an easy task in general, but for the current parameters it turns out that the transition is still observable in equilibrium simulations at finite temperature, and then we can be sure that it will persist down to zero temperature. In fact, the $v(P)$ function in constant v simulations at $T=0.09$ is also plotted in Fig. 10. We see that hysteresis upon compressing and decompressing has completely disappeared, as it should be since we are in thermodynamic equilibrium. The $v(P)$ curve has an abrupt change at $P\sim 0.75$, signaling the existence of a two phase coexistence region, and then a first-order transition.

Next we simulated a case in which the attraction is much shorter ranged, specifically, we used the attraction form (2) with $b=2.2$ and $\alpha=1.0$ (the interaction potential in this case can be seen in Fig. 1). For these parameters we are still able to detect the existence of the first-order thermodynamic transition in simulations at finite temperature. In Fig. 12 we plot the $v(P)$ curve at $T=0.09$, in which hysteresis has disappeared, and signs of a first-order transition at $P\sim 0.55$ are apparent. The compression-decompression curve at $T=0$ is shown also in Fig. 12. We see that in this case in which the attraction is much shorter ranged, the signs of global mechanical instabilities are still clearly observable. Note also that in this case, the decompression to $P=0$ (in the constant P simulations) was such that the system was not able to regain its initial density, and remains in a densified structure (in the constant volume simulations the system reaches an state of negative pressure, which of course should be considered as metastable with respect to a gaseous phase).

Let us briefly summarize the numerical results we have presented, before going to their relevance to understand the phenomenology of water and silica. For the case of no attraction between particles the $v(P)$ curve at zero temperature shows hysteresis upon compression-decompression, which is originated in local mechanical metastabilities. The thermodynamic $v(P)$ in this case is smooth and globally stable $(\partial v/\partial P<0)$. When an attraction of sufficiently long range is included, and in the case this is stronger than some minimum value we get both a thermodynamic phase transition and global mechanical instabilities at $T=0$. For attractions of shorter range, and in cases we can guarantee the existence of a first-order transition, we have observed that the global mechanical instability still exists.

IV. UNIFYING THE SILICA AND WATER PHENOMENOLOGY

Silica and water display many anomalous thermodynamic behavior. They include the well known density anomaly (a temperature at which density is maximum), compressibility and specific heat anomalies, and diffusivity anomalies. These anomalies do not require the existence of a first-order liquid-liquid or amorphous-amorphous transition to exist. In fact, basically all of them are found in the present model with no attraction, i.e., when we can be sure that there is no first-order transition [6].

Experimental and numerical evidence suggests that water possess a first-order liquid-liquid equilibrium at low temperatures. Experimental evidence of a first-order transition in silica is lacking. The present model shows that hysteresis in $v(P)$ curves is by no means a strong evidence of a first-order transition if a global mechanical instability is not observed. And in fact, experiments show that silica is globally stable upon compression and decompression, although displaying hysteretic behavior. Some numerical evidence of a first-order transition in silica has been presented. In one case, however, [12] the evidence was just the crossing of the free energies obtained during compression and decompression simulations at $T=0$ of model silica. This was erroneously attributed to an underlying first-order transition [16]. As we showed in our model this crossing occurs whether there is a first-order transition or not, and it is due to microscopic metastabilities. More serious evidence come from the simulations by Voivod *et al.* [17]. They use two different numerical models of silica and extrapolate high-temperature results to zero temperature, finding evidence of a first-order transition. Still, the results are preliminary, and based on extrapolations that call for more detailed study.

We have shown that a very simple and transparent model has or has not a first-order transition depending on the strength of the attraction that is included. We have shown simulations in which a mechanical instability at $T=0$ and a thermodynamic first-order transition exist. The mechanical instability is qualitatively similar to that found in water in experiments at $T\sim T_g$. This leads us to expect that water must display the same instability even in experiments at much lower temperatures. To confirm this expectation it would be interesting if some of the models that are used to simulate water, and that have shown liquid-liquid coexistence, were tried in the limit of zero temperature to look for the mechanical instability, or even if compression decompression experiments were done in water at much lower temperatures.

In the case of a long-range attraction between particles, we have shown that a thermodynamical first-order transition and global mechanical instabilities are closely correlated. In cases in which attraction is short ranged, and when the first-order thermodynamical transition is observable in equilibrium simulations, we have still observed global mechanical

instabilities. We have not been able to identify a set of parameters for our model where a thermodynamical transition occurs in the lack of global mechanical instabilities. But this may be due to our incapacity of detecting a thermodynamic first-order transition at very low temperatures when this transition does not show up at temperatures at which equilibrium simulations are possible.

On the basis of the present results we consider that the two possible scenarios for silica are the following. It may happen that silica does not have a first-order transition. Our results for zero or low intensity attraction correspond in fact to a case in which a first-order transition does not exist, and the phenomenology we obtain is closely related to that of silica [18]. Still, the other open possibility is in fact that silica has a first-order transition but this is not reflected in the zero temperature compression-decompression experiments. In this respect again, it would be nice if the numerical models used for silica that seem to posses a first-order transition (and in case in fact this is confirmed) were used at $T=0$ to search for a global mechanical instability. If this is obtained, then those models will be shown to be no reliable to describe silica in this limit, since we know real silica does not have this instability. If the model does not show a mechanical instability instead, this would indicate that the correlation between mechanical instabilities and a first-order thermodynamical transition is not universal.

V. SUMMARY AND CONCLUSIONS

In this work we have studied a model of a glass forming fluid, consisting of spherical particles with a hard core, a repulsive shoulder, and some amount of attraction. We investigated to what extent the existence of global mechanical instabilities at $T=0$ is correlated to the existence of a thermodynamical first-order transition between two amorphous phases. We have obtained that the model without, or with weak attraction between particles does not display a first-order transition or global mechanical instabilities. This behavior coincides with the known phenomenology of silica. In the presence of a strong attraction between particles, both a first-order amorphous-amorphous transition and global mechanical instabilities at $T=0$ were obtained. This scenario corresponds to the behavior of water. Our work suggests that the difference between the phenomenology of silica and water may be related to the lack of an amorphous-amorphous transition in silica, in opposition to the existence of this transition in water. This is not incompatible with the existence of coincident thermodynamic anomalies in both cases.

ACKNOWLEDGMENTS

This work was financially supported by Consejo Nacional de Investigaciones Científicas y Técnicas (CONICET), Argentina. Partial support from Fundación Antorchas is also acknowledged.

[1] P.H. Poole, F. Sciortino, U. Essman, and H.E. Stanley, Nature (London) **360**, 324 (1992).
[2] Y. Katayama, T. Mizutani, W. Utsumi, O. Shimomura, M. Yamakaya, and K. Funakoshi, Nature (London) **403**, 170 (2000).
[3] J.N. Glosli and F.H. Ree, Phys. Rev. Lett. **82**, 4659 (1999).
[4] O. Mishima and H.E. Stanley, Nature (London) **396**, 329 (1998), and references therein.
[5] O. Mishima, L.D. Calvert, and E. Whalley, Nature (London) **310**, 393 (1984); O. Mishima, K. Takemura, and K. Aoki, Science **254**, 406 (1991); O. Mishima, J. Chem. Phys. **100**, 5910 (1994).
[6] E.A. Jagla, J. Chem. Phys. **111**, 8980 (1999).
[7] C.A. Angell, R.D. Bressel, M. Hemmati, E.J. Sare, and J.C. Tucker, Phys. Chem. Chem. Phys. **2**, 1559 (2000).
[8] P.H. Poole, M. Hemati, and C.A. Angell, Phys. Rev. Lett. **79**, 2281 (1997).
[9] M. Grimsditch, Phys. Rev. Lett. **52**, 2379 (1984); R.J. Hemley, H.K. Mao, P.M. Bell, and B.O. Mysen, *ibid.* **57**, 747 (1986).
[10] J.S. Tse, D.D. Klug, and Y. Lepage, Phys. Rev. B **46**, 5933 (1992); W. Jin, R.K. Kalia, P. Vashishta, and J.P. Rino, Phys. Rev. Lett. **71**, 3146 (1993); D.J. Lacks, *ibid.* **80**, 5385 (1998).
[11] F. Sciortino, P.H. Poole, U. Essmann, and H.E. Stanley, Phys. Rev. E **55**, 727 (1997).
[12] D.J. Lacks, Phys. Rev. Lett. **84**, 4629 (2000).
[13] E.A. Jagla, J. Phys.: Condens. Matter **11**, 10 251 (1999); E. A. Jagla, Mol. Phys. **99**, 753 (2001).
[14] E.A. Jagla, Phys. Rev. E **58**, 1478 (1998); J. Chem. Phys. **110**, 451 (1999).
[15] Note that ''fluctuations'' present in all results shown at $T=0$ are originated in mechanical instabilities of the system, which are due to spatial inhomogeneities, and then they are not due to short simulation time. In fact in our $T=0$ simulations it can be formally considered that the simulation time is arbitrarily large, since mechanical equilibrium is achieved at each simulated point.
[16] E.A. Jagla, Phys. Rev. Lett. **86**, 3206 (2001); D.J. Lacks, *ibid.* **86**, 3207 (2001).
[17] I. Saika-Voivod, F. Sciortino, and P.H. Poole, Phys. Rev. E **63**, 011202 (2001).
[18] Experiments and simulations show that silica does not reach its original density upon compression-decompression, but remains in a densified state, which is not exactly the behavior of our model without attraction. But actually some amount of attraction exists indeed in silica, and then this effect can be easily justified with our model, even in a case in which a first-order transition is absent.